JOURNAL OF GEOPHYSICAL RESEARCH, VOL. 105, NO. A11, PAGES 25,155–25,169, NOVEMBER 1, 2000

Magnetopause motion driven by interplanetary magnetic field variations

D. G. Sibeck,[1] K. Kudela,[2] R. P. Lepping,[3] R. Lin,[4] Z. Nemecek,[5] M. N. Nozdrachev,[6] T.-D. Phan,[4] L. Prech,[5] J. Safrankova,[5] H. Singer,[7] and Y. Yermolaev[6]

Abstract. We use previously reported observations of hot flow anomalies (HFAs) and foreshock cavities to predict the characteristics of corresponding features in the dayside magnetosheath, at the magnetopause, and in the outer dayside magnetosphere. We compare these predictions with Interball 1, Magion 4, and GOES 8/GOES 9 observations of magnetopause motion on the dusk flank of the magnetosphere from 1800 UT on January 17 to 0200 UT on January 18, 1996. As the model predicts, strong (factor of 2 or more) density enhancements bound regions of depressed magnetosheath densities and/or outward magnetopause displacements. During the most prominent event, the geosynchronous spacecraft observe an interval of depressed magnetospheric magnetic field strength bounded by two enhancements. Simultaneous Wind observations indicate that the intervals of depressed magnetosheath densities and outward magnetopause displacements correspond to periods in which the east/west (*By*) component of the interplanetary magnetic field (IMF) decreases to values near zero rather than to variations in the solar wind dynamic pressure, the north/south component of the IMF, or the IMF cone angle.

1. Introduction

Processes within the foreshock can significantly modify solar wind parameters just prior to their interaction with the magnetosphere. *Sibeck et al.* [1989] reported evidence for strong (factor of 3) solar wind density variations whose extent was limited to the region immediately upstream from the Earth's bow shock. *Fairfield et al.* [1990] showed that densities and magnetic field strengths decrease when energetic particles are observed but increase when the particles are absent. Although they were not identified on the basis of greatly deflected flows, the resulting cavities of hot tenuous plasma bounded by narrow regions of cold dense plasma greatly resemble the hot flow anomalies (HFAs) reported by *Schwartz et al.* [1985] and *Thomsen et al.* [1986].

Thomas et al. [1995] reported the results of a kinetic simulation indicating that pressure variations upstream from the bow shock only perturb that boundary for a limited time before they propagate coherently downstream through the magnetosheath at the magnetosonic velocity. If so, the foreshock pressure variations may be an important cause of magnetopause motion. Both *Sibeck et al.* [1989] and *Fairfield et al.* [1990] associated foreshock cavities with compressions and rarefactions of the dayside magnetospheric magnetic field. *Laakso et al.* [1998] presented a case study indicating that the magnetopause moves outward during periods of radial IMF orientation, i.e., when the foreshock lies upstream from Earth.

To date, there has been no model for the detailed plasma, magnetic field, and energetic particle signatures expected during the passage of boundary waves driven by pressure variations generated in the foreshock. The purpose of this paper is to predict the characteristics of such magnetopause motion and then to compare these predictions with high time resolution Interball 1 plasma, magnetic field, and energetic ion observations in the vicinity of the northern dusk magnetopause. We use simultaneous Wind solar wind observations to demonstrate that both magnetopause crossings and geosynchronous perturbations correspond to variations in the IMF orientation, not variations in the solar wind dynamic pressure.

2. Conceptual Model

The IMF orientation constantly varies, connecting and disconnecting spacecraft just upstream from the bow shock to that boundary. A fraction of the solar wind ions incident on the bow shock is energized and reflected back into the solar wind along field lines connected to the bow shock. These reflected beams are unstable to cyclotron instabilities that scatter a small fraction of the ions to create a diffuse suprathermal population. Although their number density is small, the suprathermal ions contribute substantially to the thermal pressure in the region of connected IMF lines near the bow shock. The enhanced pressures cause the bundle of connected magnetic field lines to expand outward into the surrounding solar wind plasma. Densities and magnetic field strengths decrease diamagnetically within the expanding bundle but increase just outside the bundle in the region of compressed magnetic field lines unconnected to the bow shock [*Thomas and Brecht,* 1988].

Figure 1 illustrates the formation of a foreshock cavity and its subsequent interaction with the magnetosphere. In Figure 1a, a narrow slab of sunward and northward magnetic field lines first encounters the southern bow shock. Prior to the arrival of this slab, the IMF points dawnward. After the passage of the

[1]Applied Physics Laboratory, Johns Hopkins University, Laurel, Maryland.
[2]Institute for Experimental Physics, Kosice, Slovakia.
[3]NASA Goddard Space Flight Center, Greenbelt, Maryland.
[4]Space Science Laboratory, University of California, Berkeley.
[5]Department of Electronics and Vacuum Physics, Charles University, Prague, Czech Republic.
[6]Space Research Institute, Moscow, Russia.
[7]Space Environment Laboratory, NOAA, Boulder, Colorado.

Paper number 2000JA900109.
0148-0227/00/2000JA900109$09.00

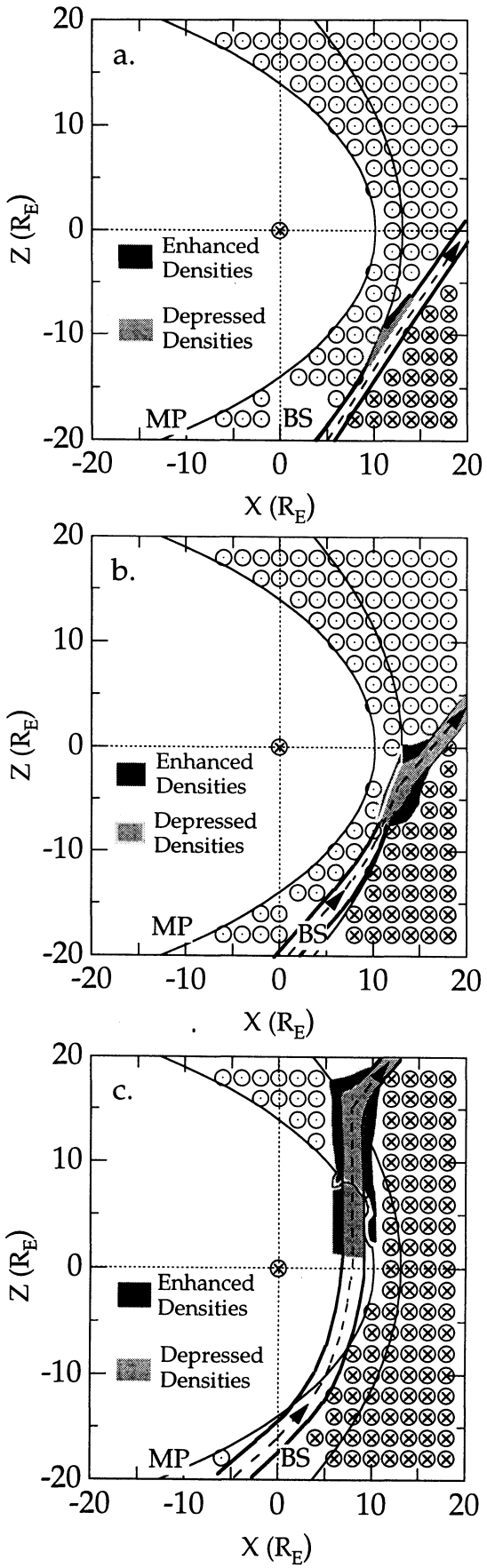

slab, the IMF points duskward. Consequently, the only upstream field lines in the noon-midnight meridional plane connected to the bow shock are those within the slab itself. As these magnetic field lines first graze the bow shock, ions are energized and reflected to stream back upstream into the solar wind. The ions depress IMF strengths and densities within the slab creating a diamagnetic cavity (light shading). The expanding cavity compresses and enhances IMF strengths and densities just outside the leading edge of the slab (dark shading).

As seen in Figure 1b, the solar wind sweeps the slab and foreshock cavity antisunward. Both the intersection of the slab with the bow shock and the foreshock cavity move northward. Ions continue to be reflected from the bow shock and scattered within the slab, creating a growing diamagnetic cavity that further compresses surrounding regions both ahead of and behind the slab. Finally, those portions of the cavity that were upstream from the southern bow shock in Figure 1a now lie downstream of that boundary: the density increases and decreases associated with the cavity have been transmitted as pressure variations into the magnetosheath.

Figure 1c depicts the subsequent evolution of the cavity and its interaction with the magnetopause. The magnetosheath flow continues to sweep the growing foreshock cavity northward and the trailing pressure enhancements bounding the cavity through the magnetosheath: around the dawn and dusk flanks and over the northern magnetopause. The pressure increases compress the magnetopause inward, whereas the decrease within the cavity allows it to expand outward. As there was no significant cavity upstream from most of the southern bow shock, there is little or no response on the southern magnetopause.

Consider the signatures spacecraft located in the vicinity of the magnetopause observe during the passage of the cavity. If the spacecraft remain within the magnetosheath, they observe the cavities as regions of depressed densities and magnetic field strengths but enhanced suprathermal particle fluxes, bounded by regions of enhanced densities and magnetic field strengths. However, the spacecraft may not remain within the magnetosheath. The depressed magnetosheath densities and pressures within the cavities permit the magnetopause to move outward past the observing spacecraft, which must then observe density increases bounding an interval of magnetospheric magnetic fields. Spacecraft located in the outer magnetosphere should exit into the magnetosheath on both sides of a region of rarefied magnetospheric magnetic field strengths. Finally, space-

Figure 1. The interaction of a slab of sunward and northward IMF lines with the bow shock and magnetopause. Prior to the arrival of the slab, the IMF points dawnward. After the arrival of the slab, the IMF points duskward. (a) The slab's first encounter with the southern bow shock is shown. The region to which reflected ions gain access, thermalize, and depress IMF densities and magnetic field strengths to form a cavity upstream from the bow shock (shown in light shading) is rather limited. As the cavity expands, it compresses the surrounding solar wind plasma, enhancing densities and magnetic field strengths (shown in dark shading). (b) The situation when the intersection of the IMF slab with the bow shock has moved northward and parts of the cavity have been transmitted through the southern bow shock is shown. A region of enhanced densities and magnetic field strengths has formed on the trailing edge of the slab. (c) The situation at a later time when the density variations associated with the slab alternately compress the magnetopause and allow it to expand outward is shown.

craft that remain within the magnetosphere should observe transient magnetic field strength increases bounding a region of depressed magnetic field strengths.

3. Data Sets

Interball 1 was launched into a highly elliptical orbit with a period of 92 hours, an apogee of 31.4 R_E and an inclination of 62.8° on August 3, 1995 [*Zelenyi and Sauvaud,* 1997]. The Interball 1 spacecraft spins with a period of 2 min about an axis oriented to within 10° of the Earth-Sun line. To achieve this accuracy, the axis is reoriented each second orbit. Interball 1 carries several Omnidirectional Plasma Sensors (VDP), which provide total flux measurements at time resolutions ranging from 1 to 16 Hz. Each VDP plasma detector [*Safrankova et al.*, 1997] measures the sum of the total ion flux and the electron flux with energies greater than 170 eV entering a wide-angle (±67°) Faraday cup. We will present observations by Interball 1's sunward-looking VDP0 detector with 1 s time resolution.

Interball 1 also carries the CORALL ion energy spectrometer [*Yermolaev et al.*, 1997] and FM 3I magnetometer [*Nozdrachev et al.*, 1998]. CORALL measures ion distribution functions within the energy per charge range 30 < E/q < 24200 eV/q via 32 energy steps in five angular sectors covering a 5° × 110° fan-shaped field of view. The centers of the sectors are oriented at look directions 42°, 66°, 90°, 114°, and 138° relative to the Earth–Sun line. Densities, velocities, and temperatures can be calculated once each 120 s spin period. We present three-component magnetic field observations by the FM 3I fluxgate magnetometer with a time resolution of 0.25 s.

The DOK 2 energetic particle experiment [*Lutsenko et al.*, 1998] onboard Interball 1 was not operating during the time interval to be considered in this paper. However, the Magion 4 subsatellite accompanies Interball 1 along its orbit, and the very similar DOKS experiment aboard Magion 4 was operating [*Kudela et al.*, 1996]. The separation vector from Magion 4 to Interball 1 during this interval was GSE (x, y, z) = (0.27, 0.30, 0.03) R_E. We present the geosynchronous magnetic field strength observed by the GOES 8 and GOES 9 spacecraft with 0.5 s time resolution [*Singer et al.*, 1996] and the solar wind observations by the 3DP plasma [*Lin et al.*, 1995] and MFI magnetic field [*Lepping et al.*, 1995] instruments on Wind with 3 s time resolution.

4. Overview of the Interball 1 Observations

Nemecek et al. [1998] reported Interball 1 and Magion 4 observations of a series of antisunward moving transient plasma flux enhancements (TFEs), each lasting from 10 s to several minutes, during the interval from 1800 UT on January 17, 1996, to 0200 UT on January 18, 1996. They attributed the TFEs to the interaction of solar wind discontinuities with the bow shock but were unable to associate those observed on this day with particular magnetic field orientations either in situ at Interball 1 in the magnetosheath or further upstream at Wind in the solar wind. We wish to show that the characteristics of the TFEs were consistent with the predictions for pressure variations generated in the foreshock described above.

As shown in Figure 2, from 1800 UT on January 17, 1996, to 0200 UT on January 18, 1996, the Interball 1 spacecraft moved antisunward along the northern dusk flank of the mag-

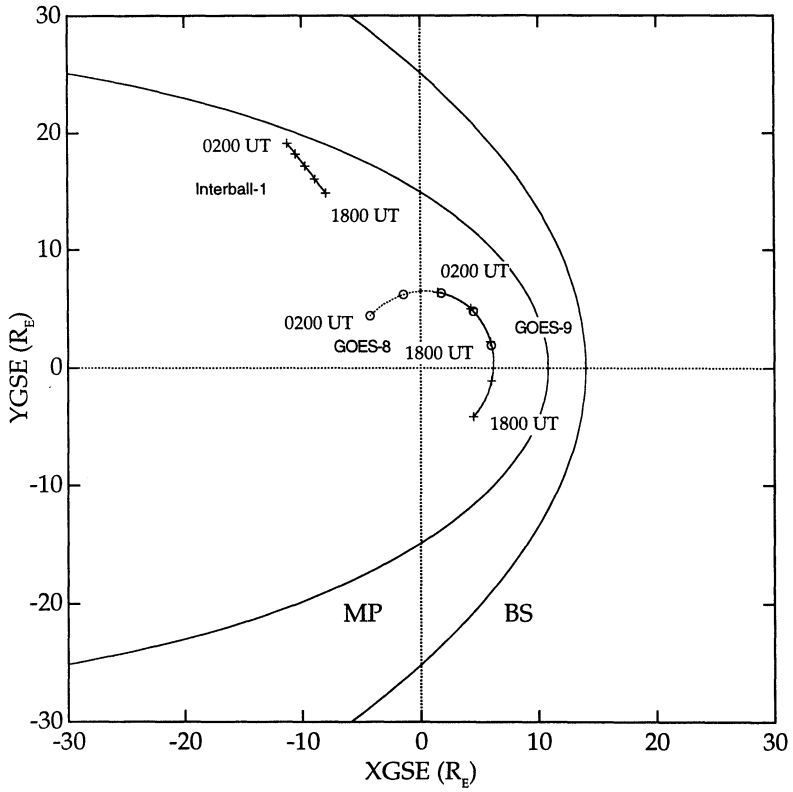

Figure 2. Interball 1, GOES 8, and GOES 9 spacecraft locations in the GSE X–Y plane from 1800 UT on January 17 to 0200 UT on January 18, 1996.

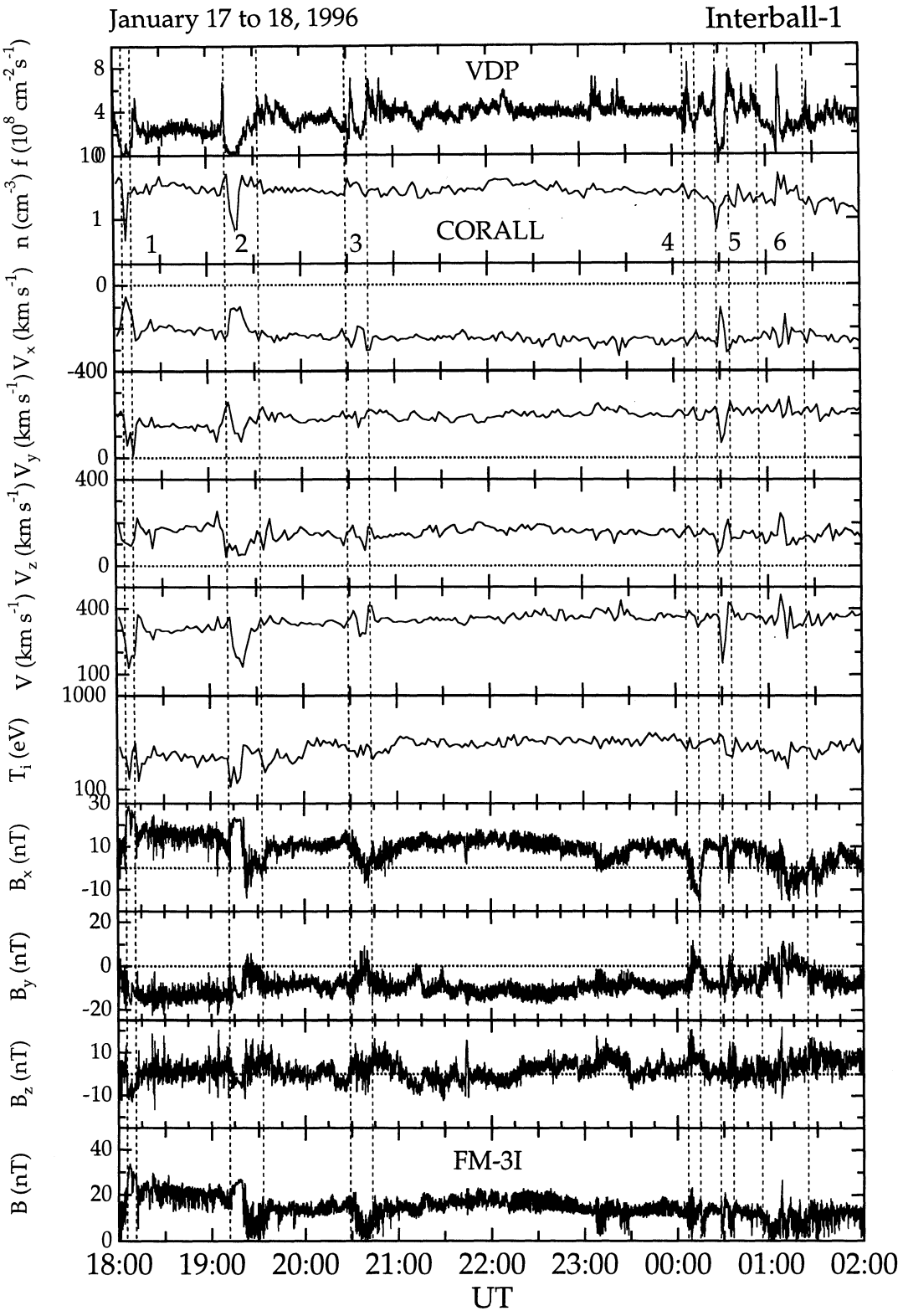

Figure 3. An overview of Interball 1 observations from 1800 UT on January 17 to 0200 UT on January 18, 1996. (Top to bottom) VDP plasma flux, CORALL ion density, velocity, and temperature, and FM 3I magnetometer observations in GSE coordinates. The spacecraft was generally within the magnetosheath. Numbered pairs of vertical dashed lines indicate six intervals when the spacecraft entered the magnetosphere and/or observed greatly reduced magnetosheath densities, fluxes, and magnetic field strengths.

netosphere from GSE (x, y, z) = (−8.0, 14.8, 12.5) to (−11.2, 19.1, 12.8) R_E. The Interball 1 plasma and magnetic field observations shown in Figure 3 indicate that the spacecraft was generally in the magnetosheath throughout this 8-hour interval. While in the magnetosheath proper, VDP measured flux levels ranging from 2 to 4×10^8 cm^{-2} s^{-1}, CORALL measured densities near 3 cm^{-3} and antisunward, duskward, and northward velocities ranging from 300 to 400 km s^{-1}. Temperatures ranged from 200 to 300 eV. The magnetometer, FM 3I, recorded high-frequency fluctuations superimposed upon a 15–20 nT background magnetosheath magnetic field that pointed sunward and dawnward.

As indicated by the numbered pairs of vertical dashed lines in Figure 3, Interball-1 encountered six periods with characteristics differing from those of the nominal magnetosheath. During periods 1, 2, and 5, VDP and CORALL observed greatly depressed densities, velocities, and fluxes bounded by enhanced densities and fluxes. FM 3I observations indicate enhanced (>20 nT) magnetic field strengths bounded by depressed (<10 nT) magnetic field strengths during each of these periods. During periods 3, 4, and 6 the VDP plasma detector and magnetometer on Interball 1 observed depressed fluxes and magnetic field strengths with occasional transient increases in the plasma flux to values exceeding those of the magnetosheath proper. CORALL, with a much lower time resolution, generally did not track these features.

There were no further VDP flux decreases during the 8-hour interval. However, there were several VDP flux increases at 2210, 2308, and 2326 UT corresponding to magnetic field strength decreases. Because these VDP flux increases were less than those attending the events in periods 1–6, and were not accompanied by any flux decreases, they will not be considered further here.

The purpose of this paper is to demonstrate that the characteristics of the six periods identified in Figure 3 are consistent with expectations for foreshock cavities swept downstream into the magnetosheath and their subsequent interaction with the magnetopause. To accomplish this task, we first examine the Interball 1/Magion 4 periods in greater detail and then inspect corresponding Wind solar wind observations.

5. High-Resolution Observations of the Magnetospheric Intervals

As shown in Figure 4, Interball 1 and Magion 4 observed a set of nested regions with distinctly different plasma, magnetic field, and energetic particle characteristics during the 30-min period from 1800 to 1830 UT. From 1806 to 1810 UT, the spacecraft pair was in the northern plasma sheet, a region marked by depressed VDP plasma fluxes (<1×10^8 cm^{-2} s^{-1}), enhanced (and spin-modulated) DOKS 60–80 keV energetic ion fluxes (>5 counts s^{-1}) and strong sunward, dawnward, and

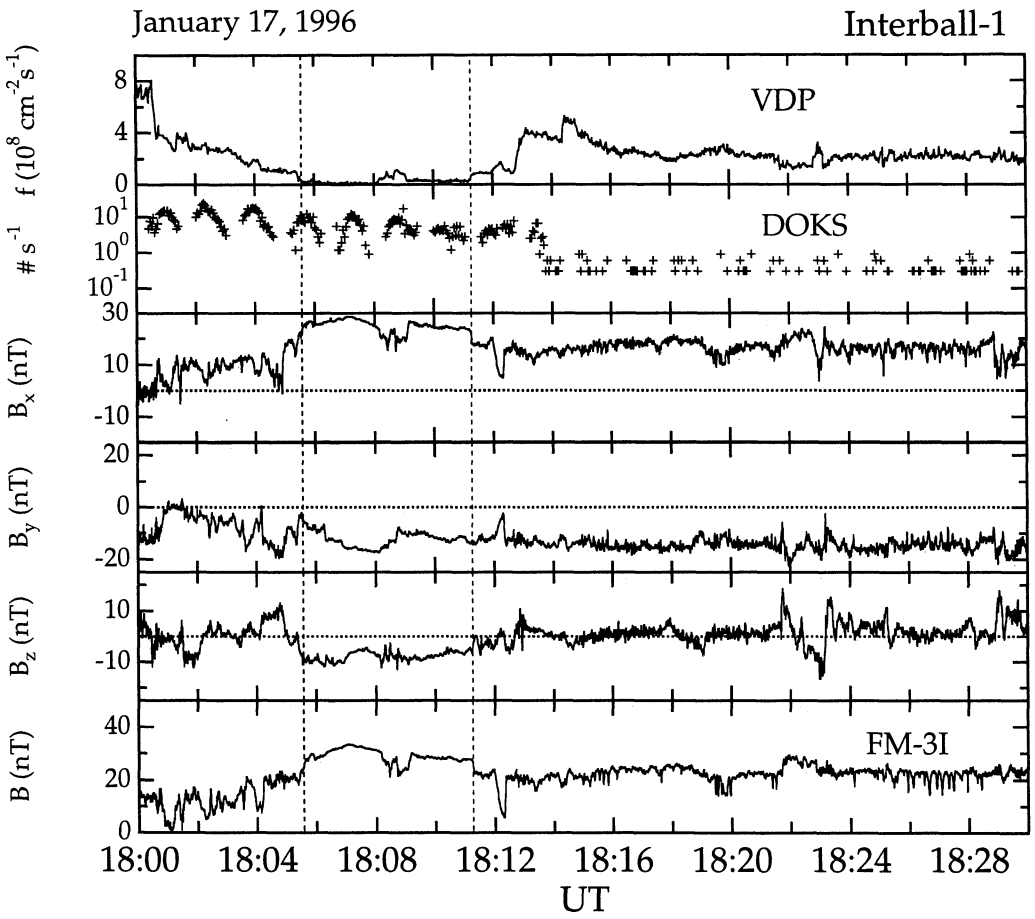

Figure 4. (top to bottom) Interball 1 VDP plasma flux, Magion 4 DOKS energetic ion (60 < E < 80 keV), and FM 3I magnetometer observations from 1800 to 1830 UT on January 17, 1996, in GSE coordinates. Vertical dashed lines bound an interval of magnetospheric observations.

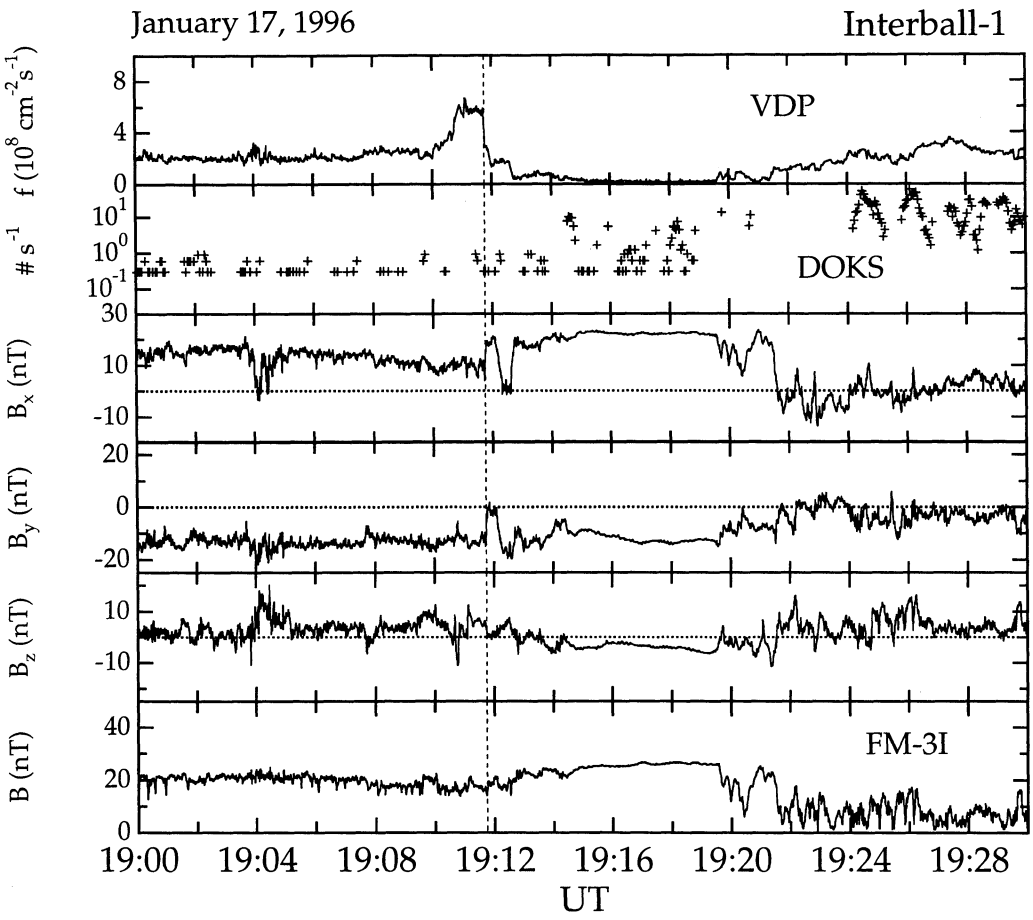

Figure 5. (top to bottom) Interball 1 VDP plasma flux, Magion 4 DOKS energetic ion (60 < E < 80 keV), and FM 3I magnetometer observations from 1900 to 1930 UT on January 17, 1996, in GSE coordinates. A vertical dashed line indicates a magnetopause crossing.

southward FM 3I magnetic fields. Just outside the magnetosphere, from 1801 to 1805 UT and at 1812 UT, the spacecraft pair observed magnetosheath-like plasma fluxes accompanied by energetic ions and weak variable magnetic fields. The *By* component of the magnetic field fell to values near zero at 1801 and 1812 UT but rose toward the magnetopause from 1801 to 1805 UT. This region was in turn bounded by one in which the plasma flux reached values greatly exceeding those seen nearby in the magnetosheath proper, i.e., 8×10^8 cm^{-2} s^{-1} at 1800 UT and almost 6×10^8 cm^{-2} s^{-1} from 1814 to 1815 UT. The *By* component of the magnetic field was large (about -10 nT) in this region. There was a data gap in the energetic ion observations at 1800 UT, but the instrument recorded fluxes at background levels from 1814 to 1815 UT. Finally, the spacecraft pair emerged into the magnetosheath proper at 1816 UT, after which they observed high VDP fluxes (>2×10^8 cm^{-2} s^{-1}), background energetic ion fluxes, and variably sunward and dawnward magnetic fields.

The observations from 1800 to 1830 UT are consistent with the predictions for a spacecraft located immediately outside the magnetopause during the passage of a foreshock cavity. Magnetic field strength and density increases bound a region of weaker magnetic field strengths, depressed densities, and enhanced energetic ion flux levels. Near the center of the cavity, pressures decrease so greatly that the magnetosphere expands outward to engulf the observing spacecraft.

Figure 5 presents Interball 1 and Magion 4 observations for the period from 1900 to 1930 UT. From 1912 to 1921:30 UT, the spacecraft were in the northern plasma sheet and lobe observing low plasma fluxes, intermittent energetic ion fluxes, and strong sunward, dawnward, and slightly southward magnetic fields. By contrast, the spacecraft were in the magnetosheath proper prior to 1910 UT, observing plasma fluxes near 2×10^8 cm^{-2} s^{-1}, no energetic ions, and sunward and dawnward magnetic fields. After 1921:30 UT, the spacecraft were again in the magnetosheath observing similar plasma fluxes but no energetic ions and a weak variable magnetic field. A large transient increase in the plasma flux to 6×10^8 cm^{-2} s^{-1} from 1910 to 1912 UT bounded the leading edge of the magnetospheric interval. There was only a modest increase in the plasma flux to 3×10^8 cm^{-2} s^{-1} on the trailing edge at 1925 UT. Pronounced decreases in the *By* component of the magnetic field at 1912:30 and after 1921:30 UT bounded the magnetospheric interval.

Overall, the observations during the 1900–1930 UT interval also coincide with expectations for a spacecraft located immediately outside the magnetopause during the passage of a pressure pulse or an HFA. The spacecraft originally lay behind the quasi-perpendicular shock and failed to observe any energetic ions. A strong increase in the magnetosheath density preceded the arrival of a region of low pressure that allowed the magnetopause to move outward. Once the magnetopause moved back

inward, the spacecraft lay behind the quasi-parallel shock, indicating that the magnetosheath/interplanetary magnetic field orientation had changed.

Figure 6 presents Interball 1 and Magion 4 observations covering the fifth period, from 0015 to 0045 UT on January 18, 1996. Prior to 0027 and after 0041 UT, the spacecraft were in the magnetosheath proper, observing plasma flux levels near 3×10^8 cm^{-2} s^{-1}, no energetic ions, and draped magnetic fields pointing sunward and dawnward. By contrast, from 0030 to 0032 UT, both spacecraft were in the northern plasma sheet observing very low plasma fluxes, energetic ions, and stronger sunward and dawnward magnetic fields. This region of enhanced magnetospheric magnetic field strengths was encompassed by one of depressed magnetosheath magnetic field strengths ($By \sim 0$), low plasma fluxes, and energetic ions from 0028 to 0030 and 0032 to 0034 UT. The By component of the magnetic field increased from 0027 to 0030 UT as the spacecraft approached the magnetopause. Sharp plasma flux increases to nearly 8×10^8 cm^{-2} s^{-1} at 0028 UT and from 0035 to 0041 UT bounded the low flux regions.

The observations from 0015 to 0045 UT are again consistent with expectations for those by a spacecraft just outside the magnetopause during the passage of a cavity or HFA. Two density increases bound a region of depressed plasma fluxes, enhanced energetic ion fluxes, and low magnetic field strengths. Presumably the depressed pressures briefly allowed the magnetopause to move outward past the observing spacecraft.

A final encounter with the magnetosphere occurred during the sixth period from 0045 to 0115 UT shown in Figure 7. Throughout most of this interval, the magnetic field was weak and variable, energetic ions were present, and the plasma flux remained at magnetosheath levels of 4×10^8 cm^{-2} s^{-1}. However, at 0107 UT, the plasma flux fell to very low values, and the magnetic field strength increased, indicating a brief encounter with the magnetosphere. This encounter was immediately followed at 0108 UT by the largest plasma flux value (8×10^8 cm^{-2} s^{-1}) seen during the 30-min period. The magnetic field orientation rotated from sunward, dawnward, and northward prior to the event to antisunward, duskward, and ecliptic orientations after the event. The observations suggest the passage of a decrease in the magnetosheath pressure followed by an abrupt increase. The presence of the energetic particles indicates that the spacecraft lay behind the quasi-parallel bow shock throughout this interval.

5.1 High-Resolution Observations of a Magnetosheath Cavity

Figure 8 presents Interball 1 and Magion 4 observations for the third period, from 2000 to 2100 UT on January 17, 1996.

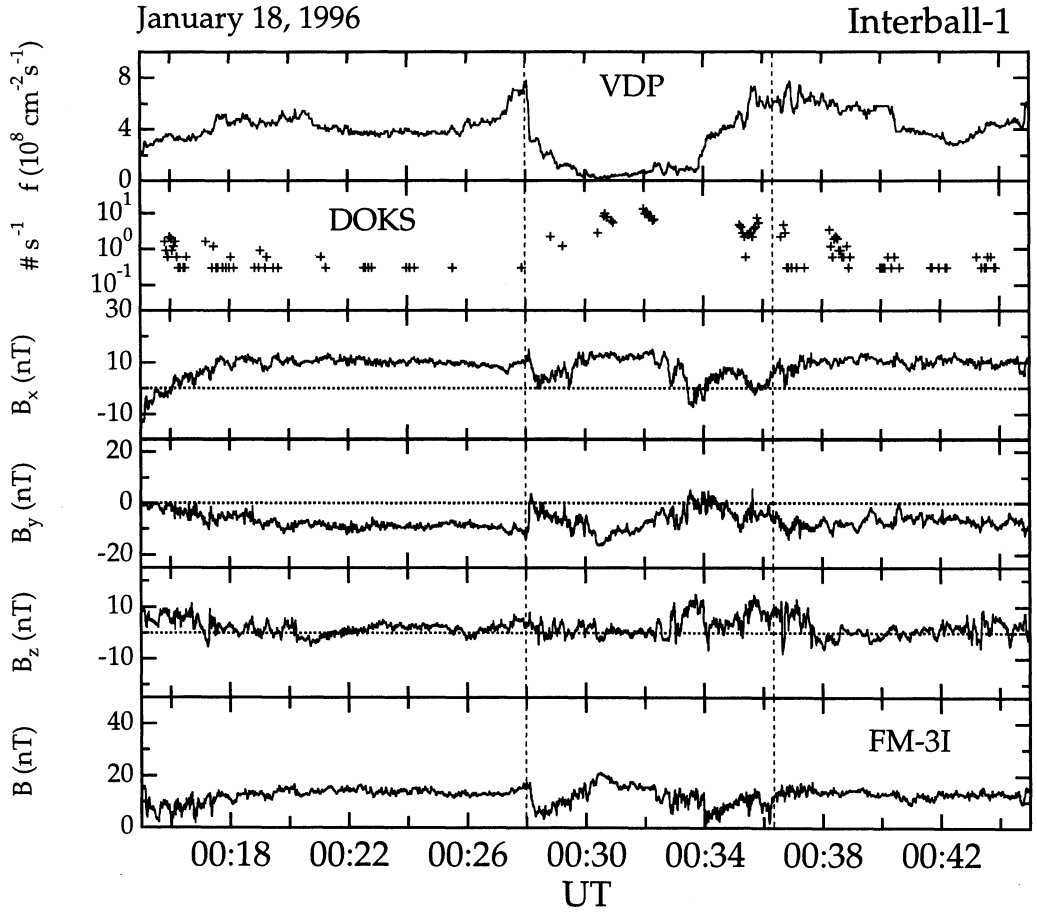

Figure 6. (top to bottom) Interball 1 VDP plasma flux, Magion 4 DOKS energetic ion ($60 < E < 80$ keV), and FM 3I magnetometer observations from 0015 to 0045 UT on January 18, 1996, in GSE coordinates. Vertical dashed lines bound an interval of depressed magnetic field strengths that in turn bound a magnetospheric interval.

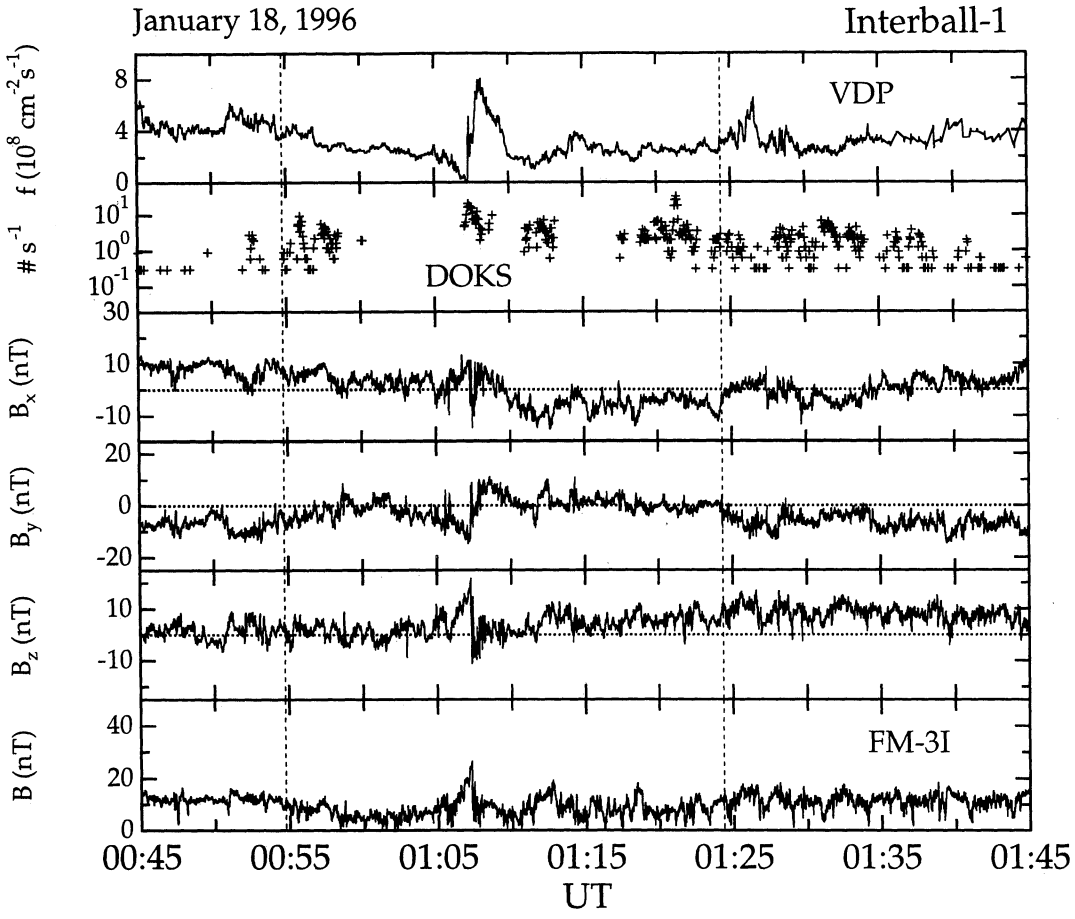

Figure 7. (top to bottom) Interball 1 VDP plasma flux, Magion 4 DOKS energetic ion ($60 < E < 80$ keV), and FM 3I magnetometer observations from 0045 to 0145 UT on January 18, 1996, in GSE coordinates. Vertical dashed lines bound an interval of depressed magnetosheath magnetic field strengths. A sharp transient decrease in the VDP flux at 0107 UT indicates a grazing encounter with the magnetopause.

As indicated by the plasma fluxes, which never fell below 1×10^8 cm^{-2} s^{-1}, the spacecraft remained within the magnetosheath at all times. Nevertheless, they observed a region of depressed plasma fluxes, weak variable magnetic fields, and enhanced energetic ion fluxes from 2035 to 2042:30 UT. Large enhancements in the plasma flux to 6×10^8 cm^{-2} s^{-1} at 2033 and 2045 UT bounded the region of depressed fluxes and field strengths. The *By* component of the magnetosheath magnetic field fell to values near zero in this region. These observations are consistent with expectations for a spacecraft that remains in the magnetosheath during the passage of a foreshock cavity. A similar sequence of events occurred during the fourth interval from 0000 to 0015 UT on January 18, which is not shown here for brevity.

5.2 High-Resolution Observations of the Magnetospheric Response

Figure 9 compares Interball 1 VDP plasma flux and GOES 8 and GOES 9 geosynchronous magnetic field strength observations for the full 8-hour interval studied in this paper. By the times of the fourth, fifth, and sixth periods, GOES 8 and GOES 9 were located near dusk, far from the dayside magnetopause. It becomes impossible to associate features at the various spacecraft, probably because the geosynchronous spacecraft begin to observe nightside magnetospheric phenomena. For example, the strong decrease in the GOES 8 magnetic field strength centered on 2245 UT and the decrease in the GOES 9 magnetic field strength at 2310 UT were associated with substorm activity.

However, the two spacecraft observed the magnetic field strength decreases bounded by enhancements predicted by the model for foreshock cavities during the first and second intervals. They observed a less pronounced decrease in the magnetic field strength just prior to the third interval. Figure 10 presents GOES 8 and GOES 9 geosynchronous magnetic field strength observations at higher time resolution for the second interval. GOES 9 (near 1030 LT at 1900 UT) observed the compressions at 1911 and 1930 UT, with a rarefaction from 1914 to 1928 UT. There was a slight compression centered on 1920 UT. By contrast, GOES 8 (near 1400 LT at 1900 UT) observed compressions at 1908, 1924, and 1931 UT, with the rarefaction from 1915 to 1930 UT. For comparison, Figure 10 (top) repeats the VDP observations of a transient flux enhancement at 1912 UT, an outward magnetopause displacement from 1913 to 1922 UT, and a gradual return to higher flux levels.

In a general sense, the features seen at GOES 8 and GOES 9 correspond to expectations for magnetopause motion induced by the passage of a cavity generated in the foreshock.

Magnetosheath density and magnetospheric magnetic field strength increases bound a cavity of depressed densities and weakened magnetic field strengths. However, the timing of the features is rather curious. One might expect compressions associated with solar wind features to sweep past the magnetosphere in a consistent manner. Instead, GOES 8 (at postnoon local times) observed the first compression before GOES 9, whereas GOES 9 (prior to local noon) observed the second and third compressions before GOES 8. Interball 1 failed to observe any clear impulsive increase in the density or flux corresponding to the second or third compressions at GOES 8 and GOES 9. We defer further consideration of this topic until section 6 of this paper, where we identify solar wind features corresponding to the events seen at GOES 8, GOES 9, and Interball 1.

6. Solar Wind Observations

Several previous studies used observations from spacecraft located directly upstream from the subsolar bow shock to demonstrate the strong relationship between pressure variations generated in the foreshock and compressions of the dayside magnetosphere. For example, *Fairfield et al.* [1990] used subsolar Ion Release Module (IRM) observations to show that the pressure applied to the dayside magnetosphere diminishes during periods of near-radial IMF and low IMF cone angles. Unfortunately, subsolar foreshock observations were unavailable for this case study, and we must instead rely upon observations by Wind. Because Wind was located far upstream and far off the Earth-Sun line near GSE $(x, y, z) = (45, -56, 5)\ R_E$, we must verify that it was an appropriate monitor for Interball-1 before attempting to identify features in the Wind observations corresponding to the Interball-1 events.

Figure 11 compares Wind interplanetary and Interball 1 magnetosheath/magnetospheric magnetic field observations for the same 8-hour interval shown in Figure 3. With the exception of the three brief intervals when Interball 1 was inside the magnetosphere (1806–1810, 1912–1921:30, and 0030 to 0032 UT), the Interball 1 magnetosheath magnetic field observations should reflect the IMF features seen by Wind. As indicated by the solid line segments in Figure 10, this was indeed the case for a number of features in the *By* and *Bz* components with durations ranging from 10 to 30 min. Although Wind was located upstream from Interball 1, it observed these features 0–15 min after Interball 1 due to the relative positions of the spacecraft and the nearly spiral IMF orientation.

While the overall trends in the *By* and *Bz* components at the two spacecraft are similar, the same cannot be said for either the *Bx* or *B* traces. In particular, there were no decreases in the Wind magnetic field strength corresponding to the decreases in the Interball 1 magnetosheath magnetic field strength at 1800, 1925, 2040, 0010, 0035, and 0100 to 0130 UT. While the comparison of the *By* and *Bz* traces demonstrates that Wind can be

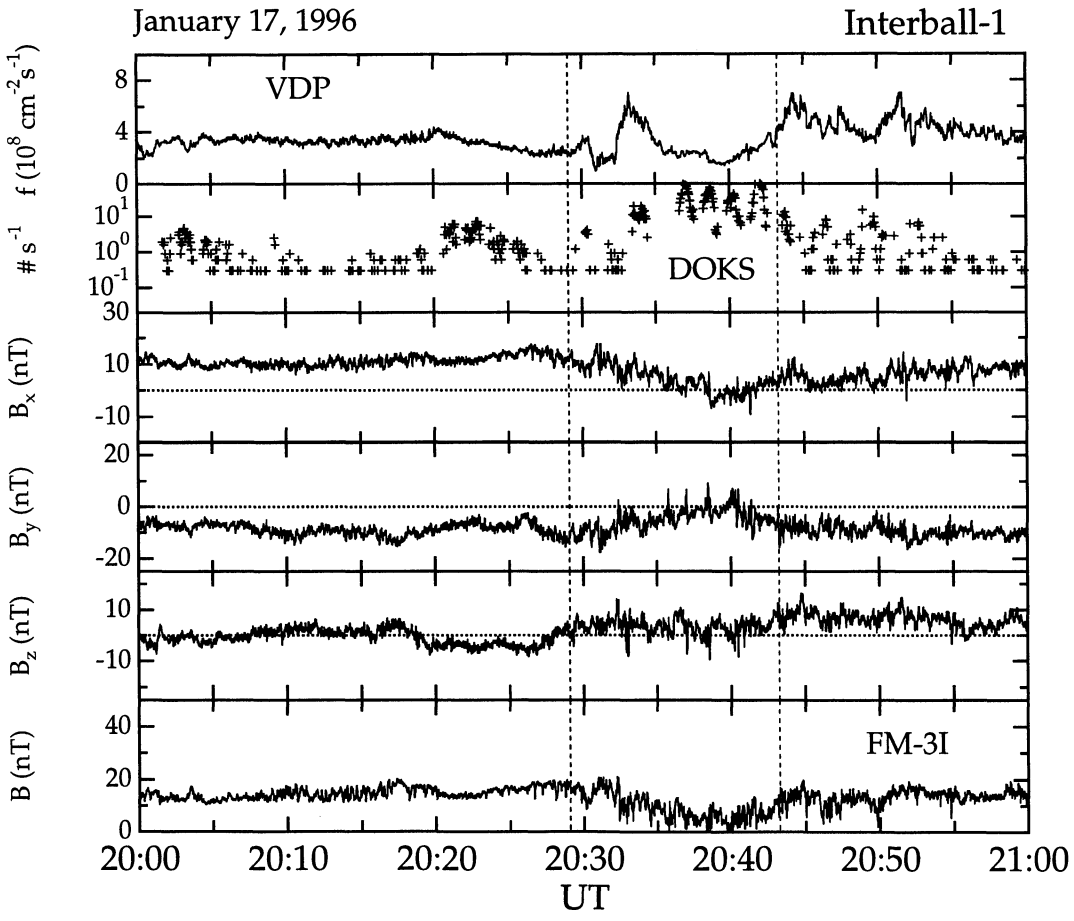

Figure 8. (top to bottom) Interball 1 VDP plasma flux, Magion 4 DOKS energetic ion (60 < E < 80 keV), and FM 3I magnetometer observations from 2000 to 2100 UT on January 17, 1996, in GSE coordinates. Vertical dashed lines bound an interval of depressed magnetosheath magnetic field strengths.

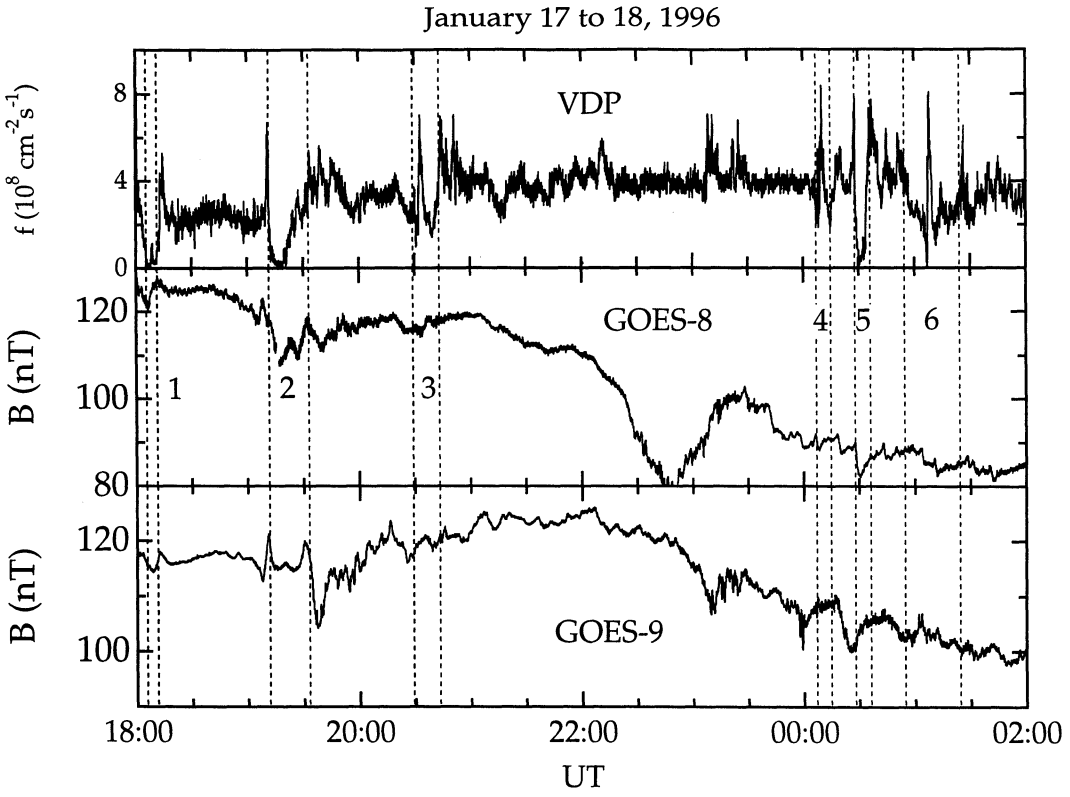

Figure 9. A comparison of Interball 1 VDP flux observations with GOES 8 and GOES 9 geosynchronous magnetospheric magnetic field strengths from 1800 UT on January 17 to 0200 UT on January 18, 1996.

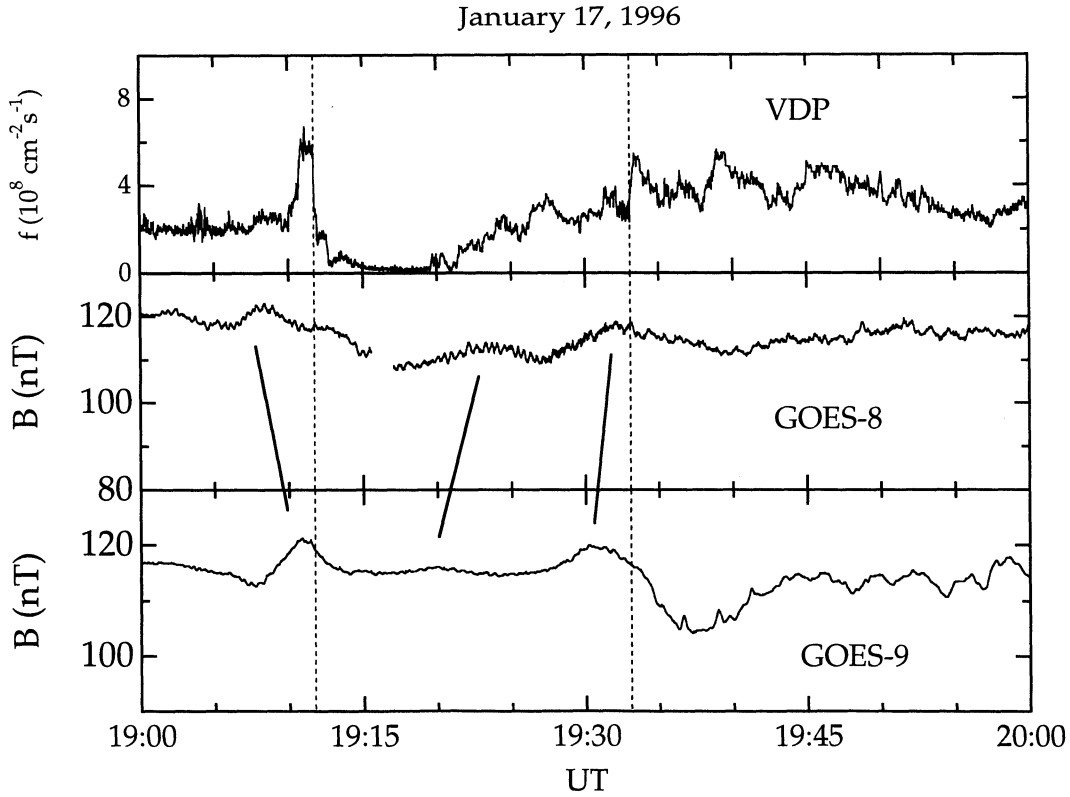

Figure 10. A comparison of Interball 1 VDP flux observations with GOES 8 and GOES 9 geosynchronous magnetospheric magnetic field strengths from 1900 to 2000 UT on January 17, 1996. Solid lines connect compressions in the GOES 8 and GOES 9 traces.

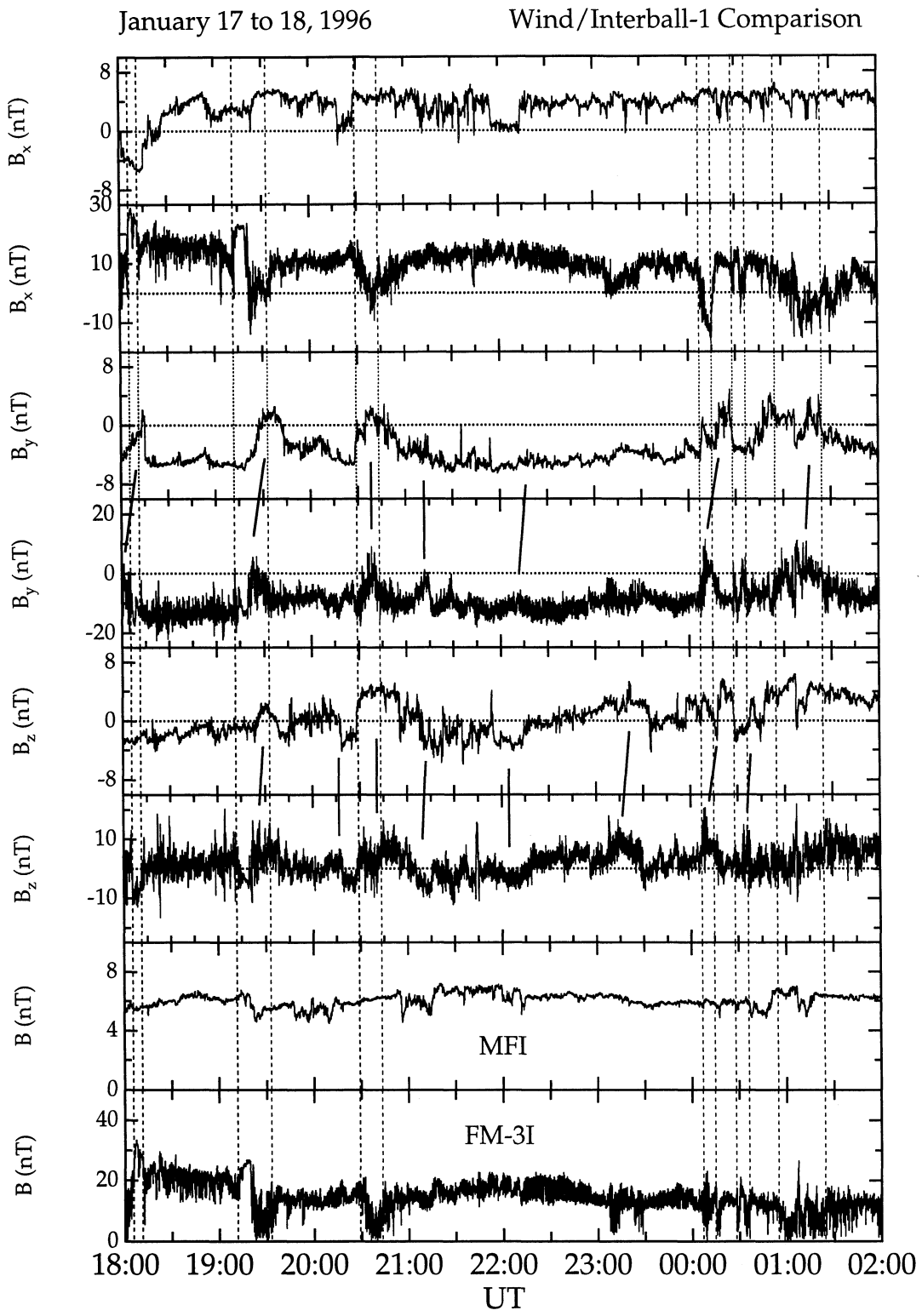

Figure 11. A comparison of Wind interplanetary and Interball 1 magnetosheath magnetic field observations from 1800 UT on January 17, 1996, to 0200 UT on January 18, 1996. Vertical dashed lines indicate six intervals during which Interball 1 either entered the magnetosphere or observed depressed magnetosheath magnetic field strengths and plasma fluxes. Solid lines connect similar features in the *By* and *Bz* traces. There are no similar features in the *Bx* and *B* traces.

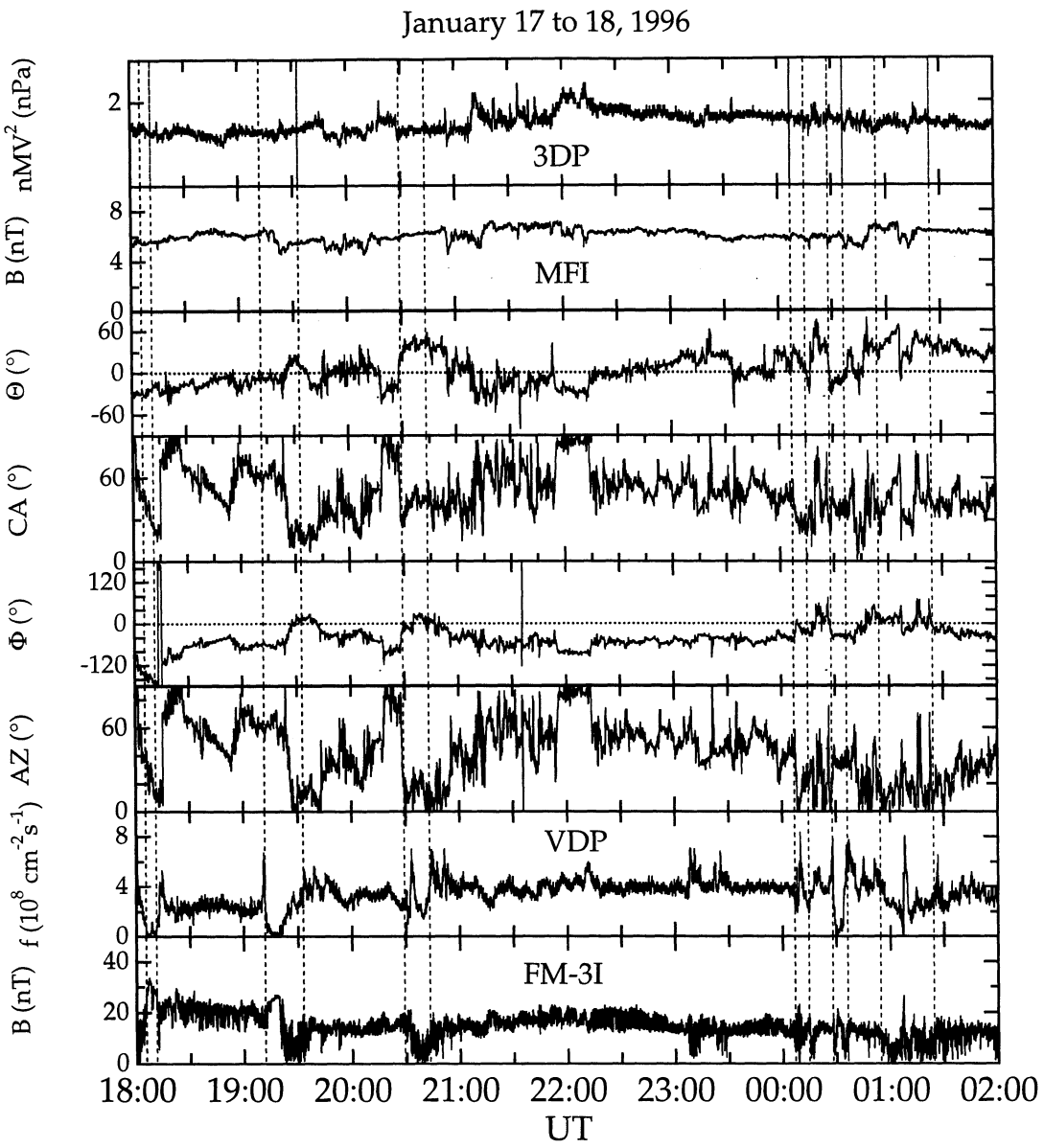

Figure 12. A comparison of Wind solar wind and Interball 1 magnetosheath/magnetospheric observations. (top to bottom) Wind 3DP observations of the solar wind dynamic pressure, Wind MFI observations of the IMF strength, latitude, cone angle, longitude, and the azimuthal angle between the IMF longitude and the Earth–Sun line, the Interball 1 VDP plasma flux, and the Interball 1 FM 3I magnetic field strength. Vertical dashed lines indicate six intervals during which Interball 1 either entered the magnetosphere or observed depressed magnetosheath magnetic field strengths and plasma fluxes.

used to monitor the solar wind input into the magnetosphere from 1800 to 0200 UT, the comparison of the total magnetic field strength traces indicates that some process in the foreshock or magnetosheath significantly modifies the solar wind shortly prior to its interaction with the magnetosphere.

To help identify this process, Figure 12 compares Wind and Interball 1 plasma and magnetic field observations. Pairs of vertical dashed lines identify six intervals in which Interball 1 observed magnetospheric and/or depressed magnetosheath magnetic fields. As Interball 1 observed a relatively constant magnetosheath velocity but flux variations ranging from 2 to 8×10^8 cm^{-2} s^{-1} on timescales of 10 to 60 s, we might expect to observe a factor of 4 variations in the solar wind dynamic pressure on similar timescales. By inspection of Figure 12 (top), we can immediately rule out the simplest explanation for the Interball 1 events, namely that they corresponded to decreases in the solar wind dynamic pressure.

Now consider the possibility that the magnetopause motion resulted from HFAs battering the magnetopause. In this case, each Interball 1 event should correspond to a single abrupt change in the IMF orientation. Figure 12 shows that there were isolated and abrupt changes in the IMF azimuth just after the first event at 1815 UT, during the second event at 1925 UT, and just prior to the third event at 2030 UT. However, there were no isolated abrupt changes in the IMF orientation at the times of the latter three events, and the fact that lag times must

range from positive to negative during the first three events diminishes the likelihood of any association between the Interball 1 events and the IMF discontinuities.

Another possibility is that southward IMF turnings eroded the dayside magnetopause inward and northward IMF turnings allowed it to move outward. However, as indicated in the third panel of Figure 12, the intervals during which Interball-1 observed magnetospheric magnetic fields do not correspond to northward IMF turnings.

Yet another possibility is that Interball 1 observed magnetospheric magnetic fields and/or depressed magnetosheath magnetic fields during intervals when Wind observed low IMF cone angles. However, the fourth panel of Figure 12 shows that this too was not the case. While the IMF cone angle was small for the first interval and became small shortly after the second interval (consistent with lag times estimated in the discussion of Figure 11), it was not small for the third interval and ranged from very large to very small during the remaining intervals. As noted by *Nemecek et al.* [1998], there was no clear correspondence between the Wind cone angle and Interball 1 ion flux.

Continuing the search for the cause of the Interball 1 magnetopause crossings and intervals of depressed magnetosheath magnetic field strength requires returning to Figure 11. As can be seen in the fourth panel of this figure, the magnitude of the *By* component of the magnetosheath magnetic field diminished each time Interball 1 entered the magnetosphere or observed depressed magnetosheath magnetic field strengths. As the short solid lines between panels 3 and 4 of Figure 11 indicate, decreases in *By* at Interball 1 corresponded to decreases in the magnitude of *By* at Wind. The combined Wind and Interball 1 observations provide evidence for an unexpected result, namely that the magnitude of IMF *By* controls the location of the flank magnetopause.

Finally, with the origin of the Interball 1 events identified, we can inspect the Wind observations to see if they provide an explanation for the lag times seen in the VDP, GOES 8, and GOES 9 event from 1910 to 1930 UT. We have just associated this event with a decrease in the *By* component at Wind from 1925 to 1938 UT. Applying minimum variance analysis [Siscoe et al., 1968] to the Wind observations yields a normal that points in the GSE $(x, y, z) = (0.26, 0.42, \text{and } -0.87)$ direction for the Wind discontinuity at 1925 UT and a normal that points toward $(0.28, -0.17, 0.94)$ for the Wind discontinuity at 1938 UT. Consequently, the first discontinuity sweeps across the Earth's bow shock and magnetopause from southern dusk to northern dawn, whereas the second discontinuity sweeps across these boundaries from northern dawn to southern dusk. The sense of the motion is precisely that required to explain the sequence of events shown in Figure 10 and discussed above, in which postnoon GOES 8 observes the leading edge of the event prior to prenoon GOES 9 and further antisunward Interball 1. By contrast, prenoon GOES 9 observes the trailing edge prior to postnoon GOES 8.

7. Discussion and Conclusions

We used previously reported observations of HFAs and foreshock cavities upstream from the bow shock to infer the characteristics of corresponding features in the magnetosheath, at the magnetopause, and inside the magnetosphere. If the solar wind flow simply sweeps the upstream features downstream, then magnetosheath events should be identifiable as diamagnetic cavities filled with a heated tenuous solar wind plasma and depressed magnetic field strengths bounded by narrow regions of enhanced densities. We reported high time resolution Interball 1 and Magion 4 observations of one such event in the magnetosheath at 2040 UT on January 17, 1996, and noted a second event at 0015 UT on January 18, 1996. *Paschmann et al.* [1988], *Schwartz et al.* [1988], and *Safrankova et al.* [2000] have reported examples of similar magnetosheath events.

The arrival of a density/pressure cavity increase bounding a cavity should cause spacecraft located in the magnetosheath just outside the dayside magnetopause to observe density increases bounding a magnetospheric interval. We identified two such intervals in the Interball 1 and Magion 4 observations of the dusk magnetopause at 1800 and 1915 UT. *Sibeck et al.* [1999] reported Geotail observations of a third event on the dawn magnetopause.

Variations in the foreshock density/dynamic pressure alternately compress and rarefy the dayside magnetospheric magnetic field strength. Pressure increases bounding a cavity should generate transient magnetospheric compressions bounding a region of reduced magnetospheric magnetic field strengths. We presented high time resolution GOES 8 and GOES 9 observations of one such event at 1915 UT. *Sibeck* [1992, Figure 6] presented Charge Composition Explorer (CCE) and IRM observations of two similar magnetospheric events at 1020 and 1040 UT on October 28, 1984. The geosynchronous observations used in the present study allowed us to demonstrate that the leading and trailing edges of the cavity swept past the spacecraft in differing directions, and we suggested that this might be consistent with past work indicating strikingly different orientations for leading and trailing edges of HFAs upstream from the bow shock [e. g., *Paschmann et al.*, 1988; *Schwartz et al.*, 1988].

We sought to identify a cause for the magnetopause motion and magnetosheath density/magnetic field variations seen by Interball1 in the Wind solar wind observations. We eliminated variations in the dynamic pressure of the pristine solar wind, fluctuations in the IMF cone angle, and north/south variations in the IMF orientation. Instead, we noted that the magnetopause moved outward during intervals when the magnitude of the IMF *By* component decreased, i.e., when the IMF longitude was nearly along or antiparallel to the Earth-Sun line. We suppose that the foreshock lay upstream from Interball 1 during intervals when IMF *By* was small but not when it was large. Magnetosheath densities and pressures diminished behind the foreshock, allowing the magnetopause to move outward during each Interball 1 event. Increases in the *By* component seen just prior to the 1805 and 0030 UT magnetopause crossings were probably caused by draping of the magnetosheath magnetic field against the magnetopause.

Magnetosheath plasma fluxes varied by at least a factor of 4 during an interval of relatively steady velocities, indicating that densities (and therefore pressures) applied to the magnetosphere also varied by a factor of 4. Pressure balance considerations allow us to set an upper limit on the amplitude of the corresponding magnetopause motion. Because densities and temperatures within the magnetosphere were low and the magnetic field strength strong (see Figure 3), the contribution of the magnetic field to the total pressure in the magnetosphere greatly exceeded that from the plasma. The magnetospheric magnetic field strength diminishes with radial distance (R) from Earth as R^{-3}, the magnetic pressure as R^{-6}. Consequently, a factor of 4 variations in the pressure applied to the magnetosphere drive ~26% variations in the magnetopause position. At

the time of the events reported in this paper, Interball 1 was located some 21 R_E from Earth, thus the potential amplitude for the magnetopause motion was ~5.4 R_E. However, because the pressure enhancements only last for 10–60 s, amplitudes of this magnitude were probably not achieved. Observed fluctuations in the magnetopause velocity on this day were of the order of 100 km s^{-1}. At these speeds, the magnetopause would move ~1 R_E in 60 s, a better estimate for the amplitude of the magnetopause motion on this day.

Because the cavities are as common as solar wind discontinuities and provide large amplitude pressure variations on timescales of 10 s to several minutes, they are at least potentially the dominant cause of magnetopause motion. Observations indicating a close correspondence between foreshock pressure variations and transient compressions at geosychronous orbit [*Sibeck et al.*, 1989; *Fairfield et al.*, 1990] suggest that there is no need to invoke any other source for dayside magnetopause motion. The fact that the motion attains greater amplitudes behind the prenoon bow shock than behind the postnoon bow shock [*Howe and Siscoe*, 1972; *Wrenn et al.*, 1981; *Rufenach et al.*, 1989; *Russell et al.*, 1997] also indicates the importance of foreshock density variations in driving the magnetopause motion. Because magnetic field lines in the outer magnetosphere map to cusp latitudes, pressure variations associated with foreshock cavities may be an important source of transient events in the high latitude dayside ionosphere, like auroral brightenings [*Sitar et al.*, 1998] and mesoscale ionospheric convection vortices [e. g., *Southwood and Kivelson*, 1990].

Finally, consider the significance of the foreshock cavities, and the kinetic processes that create them, to the overall solar wind-magnetosphere interaction. *Axford* [1964] invoked solar wind turbulence striking the magnetopause as the driving mechanism for the interaction when he presented his well-known viscous interaction model. Subsequent studies ruled out the model in part because it could not explain the observed dependence of magnetospheric and ionospheric phenomena on IMF *Bz* but also in part because estimates for the available wave power and transmission rate across the magnetopause were too small [e. g., *Verzariu*, 1973; *Hill*, 1979]. These estimates were, however, based on lower-amplitude (2–3 nT) and shorter-period (10 s) waves than those discussed in this paper. A quadrupling of the pressure applied to the magnetosphere must double the magnetospheric magnetic field strength (30 nT in this case study). While it seems unlikely that waves at the magnetopause ever dominate the solar wind-magnetosphere interaction, their contribution may become significant during periods of northward IMF orientation [*Pu and Kivelson*, 1983].

Acknowledgments. Work at APL was supported by NSF's ATM Space Weather and INT Grants 9819707 and 9515523, NASA's SR&T program grant NAG5-4679, and NASA's ISTP program grants NAG5-8030 and NAG5-7920. Work at Charles University was supported by the Czech Grant Agency under Contract 205/99/1712. NATO's Cooperative Research Grant 972312 provided support for exchange visits by the Czech, Slovak, and U.S. authors of this paper. Spacecraft positions were obtained from the NSSDC's SSCWEB service. Y. Yermolaev acknowledges INTAS grants 96-2346 and 97-1612 with gratitude.

Hiroshi Matsumoto thanks A. Nishida and another referee for their assistance in evaluating this paper.

References

Axford, W. I., Viscous interaction between the solar wind and the Earth's magnetosphere, *Planet. Space Sci., 12*, 45–53, 1964.

Fairfield, D. H., W. Baumjohann, G. Paschmann, H. Lühr, and D. G. Sibeck, Upstream pressure variations associated with the bow shock and their effects on the magnetosphere, *J. Geophys. Res., 95*, 3773–3786, 1990.

Hill, T. W., Rates of mass, momentum, and energy transfer at the magnetopause, in *Magnetospheric Boundary Layers*, edited by B. Battrick, ESA SP-148, 325–332, 1979.

Howe, H. C., and G. L. Siscoe, Magnetopause motions at lunar distance determined from the Explorer 35 plasma experiment, *J. Geophys. Res., 77*, 6071–6086, 1972.

Kudela, K., J. Rojko, J. Matisin, J. Balaz, I. Strharsky, L. Michaeli, P. Opatrny, E. T. Sarris, and K. Kalaitzides, DOKS in Project Interball: Payload description and documentation, Rep. *196*, 1–56, Inst. of Exp. Phys., Slovak Acad. of Sci., Kosice, 1996.

Laakso, H., et al., Oscillations of magnetospheric boundaries driven by IMF rotations, *Geophys. Res. Lett., 25*, 3007–3010, 1998.

Lepping, R. P., et al., The Wind magnetic field investigation, *Space Sci. Rev., 71*, 207–229, 1995.

Lin, R., et al., A three-dimensional plasma and energetic particle investigation for the Wind spacecraft, *Space Sci. Rev., 71*, 125–153, 1995.

Lutsenko, V. N., K. Kudela, and E. T. Sarris, The DOK-2 experiment to study energetic particles by Tail Probe and Auroral Probe satellites in the Interball project, *Cos. Res. Engl. Transl., 36*, 93–102, 1998.

Nemecek, Z., J. Safrankova, L. Prech, D. G. Sibeck, S. Kokubun, and T. Mukai, Transient flux enhancements in the magnetosheath, *Geophys. Res. Lett., 25*, 1273–1276, 1998.

Nozdrachev, M. N., A. A. Skalsky, V. A. Styazhkin, and V. G. Petrov, Some results of magnetic field measurements by the FM-3I fluxgate instrument onboard the INTERBALL-1 spacecraft, *Cos. Res. Engl. Transl., 36*, 251–255, 1998.

Paschmann, G., G. Haerendel, N. Sckopke, E. Möbius, H. Lühr, and C. W. Carlson, Three-dimensional plasma structures with anomalous flow directions near the Earth's bow shock, *J. Geophys. Res., 93*, 11,279–11,294, 1988.

Pu, Z.-Y., and M. G. Kivelson, Kelvin-Helmholtz instability at the magnetopause: Energy flux into the magnetosphere, *J. Geophys. Res., 88*, 853–861, 1983.

Rufenach, C. L., R. F. Martin Jr., and H. H. Sauer, A study of geosynchronous magnetopause crossings, *J. Geophys. Res., 94*, 15,125–15,134, 1989.

Russell, C. T., S. M. Petrinec, T. L. Zhang, P. Song and H. Kawano, The effect of foreshock on the motion of the dayside magnetopause, *Geophys. Res. Lett., 24*, 1439–1441, 1997.

Safrankova, J., G. Zastenker, Z. Nemecek, A. Fedorov, M. Simersky, and L. Prech, Small scale observation of magnetopause motion: Preliminary results of the INTERBALL project, *Ann. Geophys., 15*, 562–569, 1997.

Safrankova, J., L. Prech, Z. Nemecek, D. G. Sibeck, and T. Mukai, Magnetosheath response to the IMF tangential discontinuity, *J. Geophys. Res.*, in press, 2000.

Schwartz, S. J., et al., An active current sheet in the solar wind, *Nature, 318*, 269–271, 1985.

Schwartz, S. J., R. L. Kessel, C. C. Brown, L. J. C. Woolliscroft, M. W. Dunlop, C. J. Farrugia, and D. S. Hall, Active current sheets near the Earth's bow shock, *J. Geophys. Res., 93*, 11,295–11,310, 1988.

Sibeck, D. G., Transient events in the outer magnetosphere: Boundary waves or flux transfer events?, *J. Geophys. Res., 97*, 4009–4026, 1992.

Sibeck, D. G., et al., The magnetospheric response to 8-minute-period strong-amplitude upstream pressure variations, *J. Geophys. Res., 94*, 2505–2519, 1989.

Sibeck, D. G., et al., Comprehensive study of the magnetospheric response to a hot flow anomaly, *J. Geophys. Res., 104*, 4577–4593, 1999.

Singer, H. J., L. Matheson, R. Grubb, A. Newman, and S. D. Bouwer, Monitoring space weather with the GOES magnetometers, in GOES-8 and Beyond, edited by E. R. Washwell, *Proc. SPIE Int. Soc. Opt. Eng., 2812*, 299–308, 1996.

Sitar, R. J., et al., Multi-instrument analysis of the ionospheric signatures of a hot flow anomaly occurring on July 24, 1996, *J. Geophys. Res., 103*, 23,357–23,372, 1998.

Southwood, D. J., and M. G. Kivelson, The magnetohydrodynamic response of the magnetospheric cavity to changes in solar-wind pressure, *J. Geophys. Res., 95*, 2301–2309, 1990.

Thomas, V. A., and S. H. Brecht, Evolution of diamagnetic cavities in the solar-wind, *J. Geophys. Res., 93*, 11,341–11,353, 1988.

Thomas, V. A., D. Winske, and M. F. Thomsen, Simulation of upstream pressure pulse-propagation through the bow shock, *J. Geophys. Res., 100*, 23,481–23,488, 1995.

Thomsen, M. F., J. T. Gosling, S. A. Fuselier, S. J. Bame, and C. T. Russell, Hot, diamagnetic cavities upstream from the Earth's bow shock, *J. Geophys. Res., 91*, 2961-2973, 1986.

Verzariu, P., Reflection and refraction of hydromagnetic waves at the magnetopause, *Planet. Space Sci., 21*, 2213–2225, 1973.

Wrenn, G. L., J. F. E. Johnson, A. J. Norris, and M. F. Smith, GEOS-2 magnetopause encounters: Low energy (<500 eV) particle measurements, *Adv. Space Res., 1*, 129–134, 1981.

Yermolaev, Y. I., A. O. Fedorov, O. L. Vaisberg, V. M. Balebanov, Yu. A. Obod, R. Jimenez, J. Fleites, L. Llera, and A. N. Omelchenko, Ion distribution dynamics near the Earth's bow shock: First measurements with the 2D ion energy spectrometer CORALL on the INTERBALL/Tail-probe satellite, *Ann. Geophys., 15*, 533–541, 1997.

Zelenyi, L. M., and J. A. Sauvaud, Interball-1: First scientific results, *Ann. Geophys., 15*, 511–513, 1997.

K. Kudela, Institute for Experimental Physics, Kosice, Slovakia 04353.

R. P. Lepping, NASA, Goddard Space Flight Center, Greenbelt, MD 20771.

R. Lin and T.-D. Phan, Space Science Laboratory, University of California, Berkeley, CA 94720.

Z. Nemecek, L. Prech, and Safrankova, Department of Electronics and Vacuum Physics, Charles University, Prague, Czech Republic 18000.

M. N. Nozdrachev and Y. Yermolaev, Space Research Institute, Moscow, Russia 117810.

D. G. Sibeck, Applied Physics Laboratory, Johns Hopkins University, 11100 Johns Hopkins Road, Laurel, MD 20723. (david.sibeck@jhuapl.edu)

H. Singer, Space Environment Laboratory, NOAA, Boulder, CO 80308.

(Received March 13, 2000; revised July 19, 2000;
accepted July 19, 2000.)